Journal of Nuclear Materials 390–391 (2009) 835–838

Contents lists available at ScienceDirect

Journal of Nuclear Materials

journal homepage: www.elsevier.com/locate/jnucmat

Fast radiation dynamics during ELMs on TCV

G. Veres [a,*], R.A. Pitts [b], A. Bencze [a], J. Márki [b], B. Tál [a], R. Tye [b], TCV Team [b]

[a] KFKI RMKI, EURATOM-Association, P.O. Box 49, H-1525, Budapest, Hungary
[b] CRPP-EPFL, Association EURATOM-Confédération Suisse, CH-1015 Lausanne, Switzerland

ARTICLE INFO

PACS:
52.25.Xz
52.55.Fa
52.70.Kz

ABSTRACT

Total radiative powers measured by AXUV diode based bolometer cameras have been measured in lower single null, third harmonic electron cyclotron resonance (X3 ECR) heated TCV ELMing H-mode discharges. Although, the non-flat spectral response of the diodes means that total radiated powers can be in error by as much as a factor 2, with time resolution on the order of several microseconds, the cameras can resolve plasma radiation dynamics on the ELM timescale. Observations show that: (i) most of the radiation comes from the divertor and outer midplane regions, (ii) about 70% of the ELM induced radiation occurs in the first third of the ELM cycle and (iii) only a maximum of ~8% of the ELM energy is lost through radiation.

1. Introduction

Although, scaling laws now exist with which the magnitude of the total energy expelled from the plasma by an Edge localised mode (ELM) event can be roughly predicted, the question of how the energy is distributed amongst different loss channels (e.g. particles and radiation) remains open. Heat loads on first wall surfaces and divertor targets due to particle fluxes can be measured with fast infrared cameras on the ELM timescale, but radiated power losses have, up until now, not been available at such high rates. An array of 7 pinhole cameras based on fast AXUV diodes [1] has recently been installed on the TCV tokamak, providing time resolution of ~5 μs for 140 chords covering the entire vacuum vessel poloidal cross-section [2]. These diodes are sensitive to photons in the range 1 eV–100 keV (1 μm–0.01 nm), but have uneven spectral response [1,3], particularly in the plasma edge regions, where carbon radiates most strongly (TCV is an all-graphite machine). They cannot therefore be used to accurately derive the absolute radiated power during an ELM, but can throw new light on the distribution of radiation during the different ELM phases, both by inspection of the line integral chord data and from full tomographic inversions.

In an earlier study [4], we had concentrated on the qualitative redistribution of the radiation during the ELM cycle using the fast AXUV camera array. The ELM cycle was consistently found to begin with an increase in the radiation around the X-point region, followed by the appearance of a radiating lobe on the outboard midplane, and finally to a picture in which radiation around the strike points dominates. Here we extend this analysis and provide upper limit estimates for the time dependence of the total radiated power through the ELM cycle.

2. Experiments

Measurements have been made in lower single null, H-mode discharges heated with 1.5 MW of third harmonic ECRH, in which ELMs of duration ~1 ms (in terms of the full cycle for changes in the radiation distribution) are observed, each expelling on average $\Delta W_{ELM} \sim 3$ kJ (15%) of plasma stored energy at a frequency of 80–100 Hz. The precise ELM type has not yet been determined but is likely to be Type I. A detailed description of similar pulses may be found in [5]. Typical discharge parameters were: $I_p = 360$ kA, $B_t = 1.45$ T (with the ion gradB drift directed towards the X-point), $\kappa_{95} = 1.7$, $\delta_{95} = 0.3$, $q_{95} = 2.4$, central $T_e = 1.6$ keV.

Fig. 1 shows the magnetic equilibrium of the discharges studied, along with all 140 lines of sight of the 7 camera AXUV system. The high chord density, covering the entire poloidal cross-section, and the broad range of crossing angles between the line-of-sights crossing angles allows tomographic inversion with a spatial resolution of a few centimetres. All signals are digitized at 250 kHz, giving time resolution on a 4 ms timescale.

3. Results

The ELMs are known to be strongly filamentary and non-axisymmetric (at least in the main chamber) – thus for a diagnostic located in a single toroidal position, like our AXUV cameras, all ELMs are different. To look for more global trends in the time variation of the radiation distribution, this variability is eliminated here through the use of coherent averaging over many events with similar ΔW_{ELM}.

* Corresponding author.
E-mail address: veres@rmki.kfki.hu (G. Veres).

0022-3115/$ - see front matter © 2009 Published by Elsevier B.V.
doi:10.1016/j.jnucmat.2009.01.220

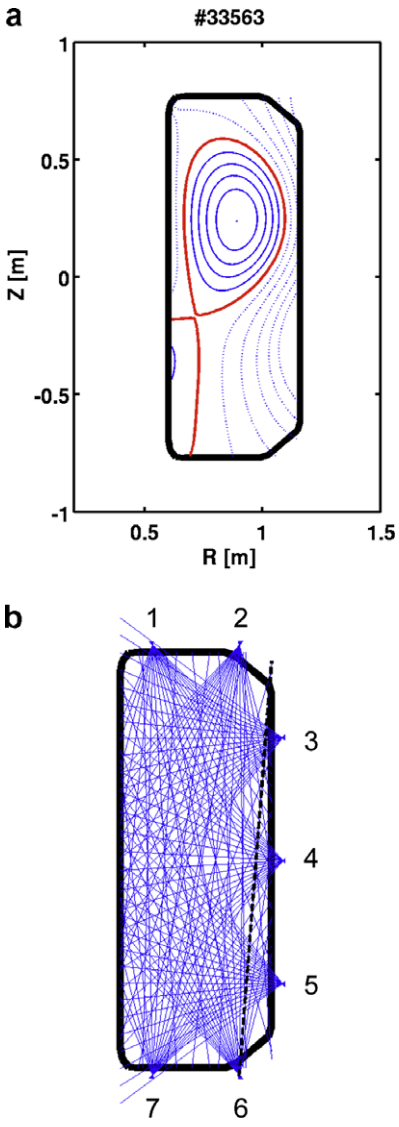

Fig. 1. (a) The magnetic equilibrium of SNL shots analyzed in the paper. (b) The lines of sight of the AXUV camera system. The AXUV reference channel (camera 6, channel 17) is marked by a dashed line.

The time base for the coherent average is taken from AXUV camera #6, channel #17 (see Figs. 1(b) and 2), where the rise of the signal is very sharp and which is consistently observed to peak first during the ELM transient. It is also a channel which does not cross the plasma core in this SNL equilibrium and it is therefore probable that the rise of the signal corresponds to the appearance of filaments in the outboard midplane vicinity (although, there is some possible overlap with ELM-wall interactions due to the finite viewing angle). A time window of ±2.5 ms around each individual ELM in the steady ELMing phase of the discharge is chosen such that its centre (t_0) coincides with the point at which the signal on channel 17 achieves 20% of its peak value. Around 30 ELMs are selected in this way and combined to produce a coherent average on a common timebase. A similar procedure is applied to the diamagnetic loop signal in order to provide a coherently averaged ΔW_{ELM}.

The signals are then spliced and averaged using these windows with $t_0 = 0$ as a reference time to which all events in coherently averaged ELM are related.

Since the ELMs are thought to be of MHD origin, it makes sense to use Mirnov signals as indicators for the ELM start and

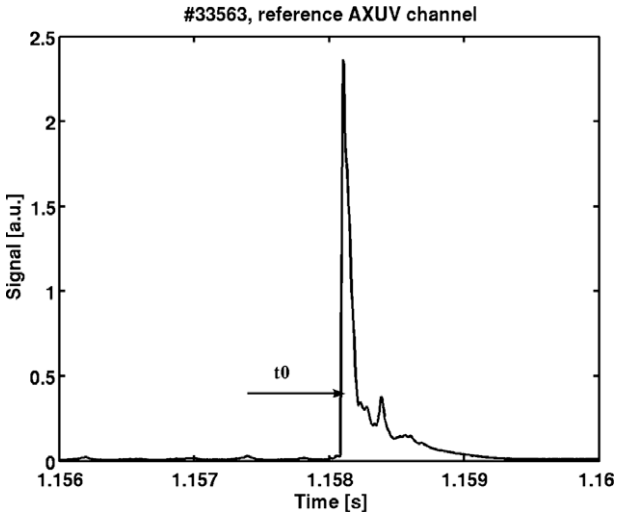

Fig. 2. The raw (not averaged) reference signal used to calculate the coherent average of ELMs. The centre of the averaging window (for this specific ELM) is marked by t_0.

thus place our reference time in the general ELM cycle, unfortunately, these signals are often extremely turbulent and unreproducible making an unambiguous definition difficult. However, a D_α signal (or the AXUV data for example) is more indicative of the arrival of the ELM at surrounding surfaces and not with the true start of the event. We have chosen to employ data from an in-vessel Mirnov coil located at the low field side (plasma) midplane, ~4 cm from the separatrix and in the same toroidal location as the AXUV camera array. After coherent averaging of the signal in the manner described above for the AXUV data, the Mirnov signal is bandpass filtered in the interval 5–25 kHz and the power (square of the signal) estimated in this frequency range. The ELM start is then identified as the time at which the power amplitude reaches 10% of its maximum. The ELM start is determined in this way to be at −40 μs.

Fig. 3 shows a series of tomographically inverted images taken at time instances −30, −20, −10 and 0 μs. At the ELM onset, the radiating zone present in the inter ELM phase around the X-point begins to move towards the inner divertor strike point (or alternatively the radiation simply begins to increase in the strike point region). Shortly afterwards, a strong radiating belt appears in the vicinity of the outboard midplane wall. This latter radiation increase is believed to be due to the appearance of filaments in the scrape-off layer and determines the zero of our time scale.

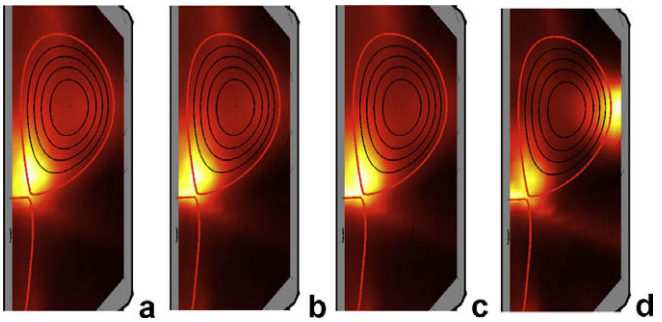

Fig. 3. Tomographically inverted images taken at times −30, −20, −10 and 0 μs, respectively, before the AXUV reference time.

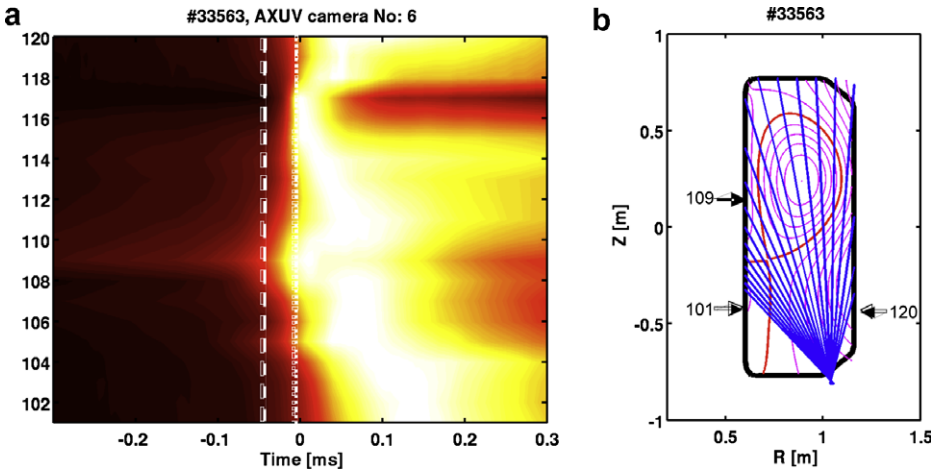

Fig. 4. (a) Contour plot of signals of camera #6 during the averaged ELM (for LOS see subplot) The dashed line shows the Mirnov reference time. (b) Lines of sights of camera #6.

In addition to the tomographic inversions, useful information can also be obtained from the line integrated (raw) data. Contour plots using these line integrals from AXUV cameras #6 and #7 (both looking at the plasma from the bottom of the chamber) are presented in Figs. 4 and 5. For ease of visualization the data from all channels are normalized to their corresponding maxima. The dashed lines on the figures identify the Mirnov ELM start. It is evident from these plots that the radiation in the X-point region begins to increase before this start time.

Examination of the time delays between the appearance of the radiation in the vicinity of the outer main chamber wall surfaces (dotted line on the Figures, channels 119 and 120 of camera #6, and channels 138 to 140 of camera #7) and the Mirnov ELM start time indicates, that the ELM filaments are formed early in the ELM cycle and propagate to the wall with radial speeds of order 2 kms^{-1} (the delay is 40–50 μs and the distance from the plasma is ~0.1 m). After filament formation, interactions at the strike points occur on timescales corresponding to the propagation of particles along the magnetic field at the acoustic speed (based on pedestal parameters) from an upstream release point (see at channel looking at the strike points on Figs. 4 and 5). Because the distance to the wall is much shorter (i.e. a few centimetres cross field) compared with the ~15 m along the field, even though the filaments are traveling at only a few percent of acoustic speed, they arrive at the walls very quickly.

The total radiated power emitted by the plasma during the coherently averaged ELM can be computed from the tomographic inversions. Fig. 6 illustrates the time evolution of the total released energy via radiation (up to the time shown on the *x*-axis) together with the total loss in the stored energy. Accounting in an approximate way for the non-flat spectral response of the diodes, what basically means that an average 0.24 A/W power-to-current coefficient was used, as suggested in [3], it appears that only ~8–15% ΔW_{ELM} is lost via radiation. For these TCV ELMs at least, the majority of the loss occurs in the outer midplane region early on in the ELM cycle, i.e. ~75% of the total radiative loss occurs during the first third of the total stored energy decrease. One possible explanation for these relatively low fractional radiated energies (which have been observed, for example to be ~50% of ΔW_{ELM} in JET [6]) is the low recycling nature of the TCV divertor plasmas in these low density third harmonic ECR heated H-modes. Even if a considerable amount of carbon is released in the ELM

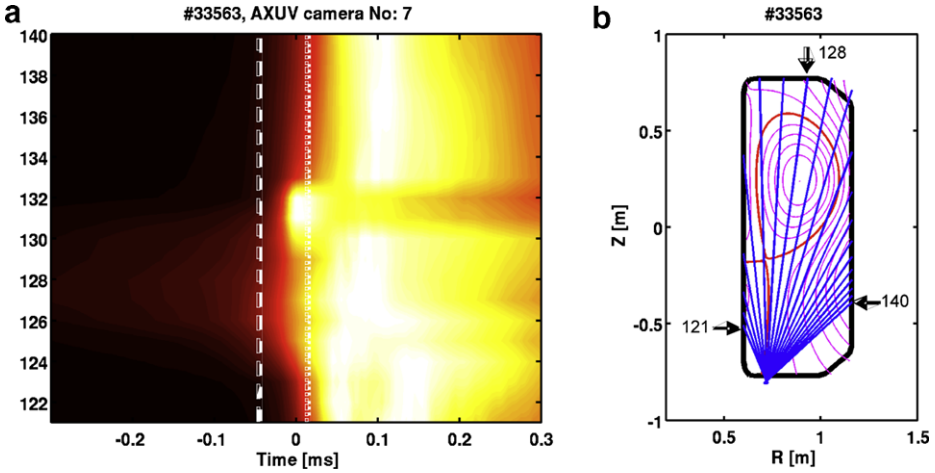

Fig. 5. (a) Contour plot of signals of camera #7 during the averaged ELM (for LOS see subplot) The dashed line shows the Mirnov reference time. (b) Lines of sights of camera #7.

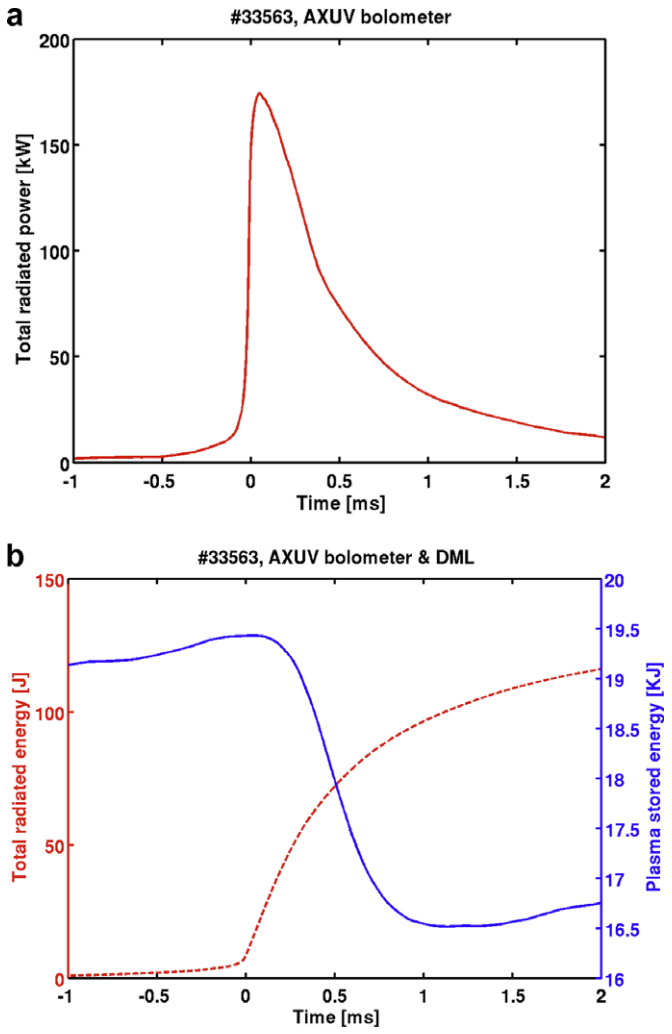

Fig. 6. (a) The radiated power calculated for the average ELM. (b) The radiated energy (left axis) compared to the loss in the plasma stored energy (right axis).

cycle, it cannot effectively radiate in the high divertor plasma temperatures.

4. Conclusion

The AXUV camera system on TCV had been proved to be an excellent (and unique) tool for tracking the time evolution of the plasma radiation during ELMs, revealing previously undetected details in radiation pattern changes. There is a striking evidence that already around the start of the nonlinear MHD phase the radiation begins to increase in the X-point vicinity. The origin of this phenomenon is not clear. One possibility is the occurrence of an X-point MARFE, but the target plasma studied here, with n/n_{GW} only $\sim$0.25, makes this unlikely.

As much as 30% of the radiation is seen in the ELM rise phase (see Fig. 3) and is localized in the outboard midplane, indicating that the early phase radiation occurs as a result of filament impact at the vessel walls. The remainder is produced when the acoustic pulse traveling parallel to the SOL field lines arrives at the divertors.

Only a comparatively low fractional energy loss due to radiation (only 8–15% of ΔW_{ELM}) is observed during these X3 ELMs. This may be due to the low recycling (i.e. high divertor temperature) nature of the low density target plasma, making it hard for any released carbon to radiate efficiently.

Acknowledgment

This work was supported in part by the Swiss National Science Foundation and EURATOM.

References

[1] http://www.ird-inc.com.
[2] A.W. Degeling, H. Weisen, A. Zabolotsky, et al., Rev. Sci. Instrum. 75 (2004) 4139.
[3] R.L. Boivin, J.A. Goetz, E.S. Marmar, et al., Rev. Sci. Instrum. 70 (1999) 260.
[4] G. Veres, R.A. Pitts, B. Gulejova et al., in: 34th EPS Conference on Plasma Physics, Warsaw, 2–6 July 2007, ECA, vol. 31F, 2007, p. 2.141.
[5] L. Porte, S. Coda, S. Alberti, Nucl. Fus. 47 (2007) 952.
[6] Pitts et al., J. Nucl. Mater. 390–391 (2009) 755.